International Journal of Scientific Research in Engineering and Management (IJSREM)
Volume: 09 Issue: 10 | Oct - 2025 SJIF Rating: 8.586 ISSN: 2582-3930

Real-Time Vibration Isolation Strategies for Vision-Based Agricultural Drones Using Optical Flow and Spectral Analysis

Guhan Srinivasamoorthy, Pavan Pradeep[1]

[1]*Department of Mechanical Engineering, Amrita School of Engineering, Coimbatore, Amrita Vishwa Vidyapeetham, India*

**Corresponding Author : cb.en.u4are21014@cb.students.amrita.edu*

---***---

Abstract - Unmanned Aerial Vehicles (UAVs) and computer vision based systems are widely used for real-time crop health monitoring in precision agriculture. However, the vibration-induced image blur is still one of the difficult problems for the automatic detection algorithms. A comprehensive evaluation of five mounting methods of the camera for the vibration damping in a lightweight agricultural drone is demonstrated. Based on real-world flight testing over cotton fields, we evaluated the performance of various isolation strategies in terms of Lucas-Kanade optical flow and Fast-Fourier Transform (FFT) spectral analysis. From basic bar to our latest double bar design rubber mounts to cush drive rubber mounts, the evolution denied several other options. The results indicate that the two-stage vibration dampers led to reduction of 88% in peak vibration amplitude of the baseline and enhanced the object detection of YOLOv10s by 53% to 88.5% mAP@50 in the nutrient deficiency identification. These results present useful guidelines for practical use of robust vision-based agricultural monitoring systems under actual field conditions.

Keywords: Precision agriculture, UAV vibration isolation, optical flow analysis, spectral analysis, computer vision, crop monitoring

1.INTRODUCTION

Precision agriculture has become a lynch pin in contemporary sustainable agriculture, focusing on data-driven methods for monitoring and improving crop health, optimizing resource allocation, and maximizing yield. Drones, or Unmanned Aerial Vehicles (UAVs), are crucial in this sense, as they can quickly survey a wide stretch of the agricultural land, and provide high perfection images with which detailed analysis on the plant status can be carried out (Barburiceanu et al., 2021; Qu & Su, 2024). When integrated with on-board deep learning models, these airborne platforms make it possible to detect and classify crop deficiencies, diseases, and anomalies in real-time with little to no human intervention (Kumar et al., 2024; Alanazi, Wahab & Al-Rimy, 2024).

The negative impact from mechanical vibration generated during the flight has been the long-standing issue of a UAV imaging system. Vibrations generated by the rotation of the engines, turbulence in the rotors and disturbances in environment (e.g. wind gusts) are transmitted to the drone frame and generate motion blur and frame instability in the onboard camera system (Kalman & Bucy, 1961; Yacef et al., 2017). These artifacts deteriorate the quality of the image data and subsequently undermine the precision of computer vision-based detectors. In Agri farming applications, nutrient deficiency conditions can manifest in mild leaf colorations or shape deformation signals, and any slight visual distortion could lead to misclassification or miss to detect for the early intervention for precision farming (Scaramuzza & Fraundorfer, 2011; Meier et al., 2012).

One of the common ways of reducing vibration in flying platforms is by the use of motor balancing, EIS, 2-axis or 3-axis mechanical gimbals (Herissé et al., 2011; How et al., 2008). These systems work, but are unsuitable for low cost, size, weight, and power constrained small UAVs. As such, it is urgent to assess the lightweight, low-cost and structurally-simple substitutes that could allow viable vibration isolation without hindering the endurance in flight or the system stability (Bachrach, He & Roy, 2009; Weiss, Scaramuzza & Siegwart, 2011).

This paper develops a comparative analysis of 5 alternatives of camera stabilization and vibration control mechanisms for a small, lightweight agricultural drone configuration aiming to reduce vibration-induced degradation of captured images. By relating vibration features with object detection models (YOLOv8 and YOLOv10s) visual performances, this study determines best camera installation and mounting configurations for real-time and drone-based plant health monitoring. The results have practical implications for UAV manufacturers as well as those interested in deploying such robust vision-based systems in real-world field settings.

2. RELATED WORK

2.1. Vibration Isolation in UAV-Based Imaging Systems

The introduction of Unmanned Aerial Vehicle (UAV) in precision agriculture requires the development of on-board sensing systems. Yet, vibrations of the drone due to operation motor dynamics, air gusts and motor resonances are sources of significant concern to image stability (Tournier et al., 2006; Bouabdallah, Murrieri & Siegwart, 2004). These low frequency vibrations can cause disruptions on image quality, which lowers the efficiency of computer vision algorithms for crop surveillance.

Active sideband control techniques have been developed to reduce these effects, along with passive methods, like rubber dampers and foam pads. The author (Görmüş, Adın & Yayla, 2023) proposed a passive vibration isolator for small UAVs, and verified the attenuation of high-frequency oscillations without significant increasing the weight. In the same way, the use of EPDM foam pads has been demonstrated to reduce specific vibration frequencies, improving image quality during flight operations (Shi, 1994).

Active type vibration isolation systems have also been examined. (Lee et al., 2017) introduced an active vibration isolation scheme for camera mounted on drones, which are actuated to cancel the vibration as it occurs. Although very effective, these systems could introduce additional complexity and power consumption, inducing them less in tune for lightweight agricultural drones (Bruhn, Weickert & Schnörr, 2005).

2.2. Optical Flow-Based Vibration Analysis

Optical flow methods have been used extensively to estimate motion and study vibration's in the context of UAVs (Liu, 2009; Sun, Roth & Black, 2010). In particular, the Lucas-Kanade method provides a computationally efficient way to track feature points across frames, and this can be exploited to measure inter-frame displacements created by vibrations.

The Author (Cai, Liu & Kou, 2021) proposed a real-time optical flow based video stabilization algorithm for UAV with significant video stability enhanced without additional hardware. Commonality with low-resolution Students They also highlights the possibility of applying software on the vibration-like image degradation.

In addition, optical flow has been combined with other sensor data. Author (Xu et al., 2025) proposed a deep neural network that combines optical flow and gyroscope data to perform video stabilization in an unsupervised fashion. This fusion mode improves the anti-interference capacity of vibration analysis for dynamic flight (Weinzaepfel et al., 2013; Dosovitskiy et al., 2015).

2.3. Spectral Analysis for Vibration Characterization

Spectral analysis, especially using the Fast Fourier Transform (FFT), gives access to the frequency components of vibration which are detrimental to the UAV imaging systems (Smith, 1997; Proakis, 2007). By determining dominant frequencies of vibration, focused interventions can be explored.

The effectiveness of FFT for identifying the UAV-induced vibrations have been highlighted through the studies. Yousaf et al., (Yousaf et al., 2017) used FFT for vibration analysis in UAV imagery and this helped designing compensation methods to improve image stabilization. Recent developments in the frequency domain analysis have made more advanced vibration characterization approach available for the small UAV platforms (Simon, 2006; Kay, 1993).

2.4. Gaps in Current Research

Although considerable efforts have been realized in the hardware and software-based vibration compensation methods in recent years, there are few studies which comprehensively combine the above methods for the real-time agricultural monitoring (ul Haq et al., 2021). In particular, the integration of both passive isolation and optical flow and spatial analysis techniques in the context of UAV-based crop health monitoring calls for future investigation.

3. METHODOLOGY

3.1 Experimental Setup

3.1.1 Vehicle Platform Selection and Configuration

The experimental vehicle utilized in this study was a customized quadrotor unmanned aerial vehicle (UAV) built upon the DJI F450 platform frame. The F450 frame was selected as the foundation for the experimental platform due to its superior structural rigidity and exceptional ease of modification, making it an ideal candidate for research applications requiring custom sensor integration and payload mounting.

3.1.2 Platform Specifications

The DJI F450 frame exhibits the following technical specifications that contributed to its selection for this research:

Structural Characteristics:

- Wheelbase: 450mm, providing optimal stability and maneuverability balance
- Construction material: Glass fiber reinforced with polyamide nylon composite, ensuring high strength-to-weight ratio
- Total frame weight: 280g (±20g manufacturing tolerance)
- Color scheme: White and black composite finish

Mounting and Integration Features:

- Standardized mounting holes with diameters of 3mm and 4mm, facilitating secure attachment of various components and sensors
- Modular design architecture enabling straightforward customization and component integration

Performance Parameters:

- Maximum All-Up Weight (AUW): 1.8kg, providing substantial payload capacity for experimental equipment
- The lightweight frame construction (280g) allows for a payload capacity of approximately 1.52kg when accounting for standard propulsion and control systems

The combination of structural integrity, modification flexibility, and adequate payload capacity made the F450 platform particularly suitable for the experimental requirements of this study. The frame's proven reliability in research applications and its compatibility with standard UAV components further supported its selection as the foundational platform for the customized experimental vehicle (Figure 1).

3.1.3 Vehicle Configuration

The quadrotor configuration was implemented to provide stable flight characteristics essential for precise data collection and experimental repeatability. The 450mm wheelbase offers an optimal compromise between agility and stability, while the composite construction ensures durability under varied experimental conditions.

Figure 1: *Frontal view showcasing the structural components and wiring configuration*

Propulsion included four brushless DC motors with 10 inch propellers, powered by a 4S LiPo battery. The utilized flight controller was the Pixhawk 4, designed by Holybro, based on high-performance processor and sensor systems. The Pixhawk 4 is powered by an STM32F765 32-bit ARM Cortex MO running at 216 MHz, with flash memory of 2 MB and RAM of 512 KB. It incorporates dual IMUs (ICM-20689 and BMI055), a barometer (MS5611), and a magnetometer (IST8310), which work in tandem to ensure accurate and stable flight throughout every mission.

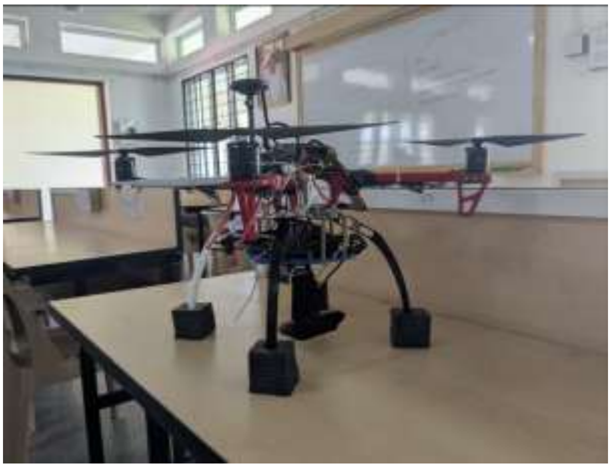

Figure 2: *Frontal view showcasing the structural components and wiring configuration.*

An NVIDIA Jetson Orin Nano was installed for on-board processing, which provided enough computation resource for image processing and deep learning inference to run in real-time (Figure 2). The primary imaging device used was a Logitech C920 HD camera, selected for its trade-off of image quality and weight. The camera was connected to the Jetson module through USB 3.0 for high speed data transfer with minimal delay.

3.2 Vibration Isolation Configurations

Five distinct camera mounting configurations were evaluated to assess their efficacy in mitigating vibration-induced image degradation. Each configuration represents a different approach to isolating the camera system from the inherent vibrations generated by the quadrotor's propulsion system.

3.2.1 Baseline Configuration (No Isolation)

The baseline configuration served as the control setup, where the camera was rigidly affixed to the front of the drone frame without any damping materials. This configuration provided the reference point for evaluating the effectiveness of subsequent vibration isolation methods (Figure 3).

Figure 3: Baseline camera mount configuration showing rigid attachment to UAV frame

3.2.2 Angled Front Mount Configuration

Similar to the baseline setup, the camera was mounted on the front of the UAV frame but oriented at a 45-degree downward angle. This configuration was designed to investigate the impact of angular placement on vibration transmission while maintaining direct frame attachment (Figure 4).

Figure 4: Angled front mount configuration with 45-degree downward camera orientation

3.2.3 Central Mount with Prop-Wash Shielding

The camera was centrally positioned on the drone's frame and equipped with protective shielding to minimize aerodynamic disturbances from direct propeller airflow. This configuration aimed to reduce both mechanical vibrations and aerodynamic-induced instabilities by positioning the camera at the geometric center of the platform (Figure 5).

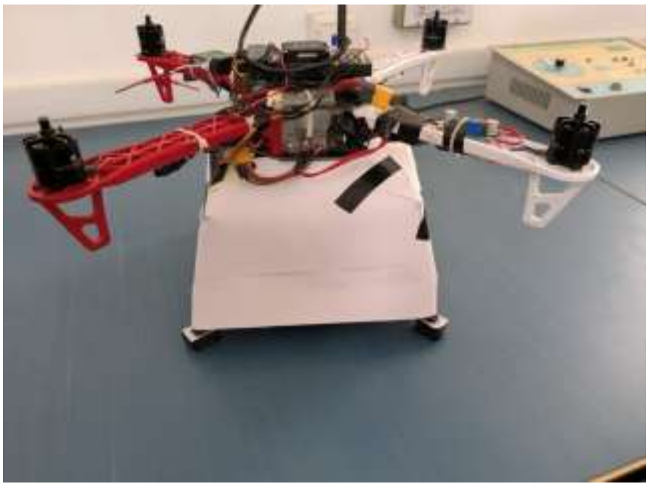

Figure 5: Central camera mount with integrated prop-wash shielding system

3.2.4 EPDM Foam Interface Configuration

Building upon the central mount design, this configuration incorporated a layer of Ethylene Propylene Diene Monomer (EPDM) foam between the camera and the mounting surface. The EPDM foam layer, strategically placed between the camera and the central mount, serves as a passive vibration damping mechanism to enhance image stability during flight operations (Figure 6).

Figure 6: EPDM foam interface setup showing passive vibration damping layer

3.2.5 Dual-Stage Vibration Dampers Configuration

This configuration incorporated two stages of rubber dampers beneath the centrally mounted camera, designed to attenuate a broader range of vibrational frequencies. The system utilized elastomeric vibration dampers that mechanically decouple the camera module from frame vibrations by absorbing high-frequency shocks and oscillations (Figure 7).

Figure 7: Dual-stage vibration damper setup with elastomeric isolation system

3.3. Data Acquisition Protocol

Flight trials were performed in a cotton field in Coimbatore, Tamil Nadu, India, under clear weather conditions and without excessive wind in order to avoid any environmental variability in the daylight time. For each configuration:

- **Flight Time**: Around 10 minutes when it was performing all the stunts including hover, ascend, descend and left / right side fly.
- **Information Collected**: High-definition video at 30 frames a second along with IMU data from the flight controller.
- **Ground Truth:** Physical markers were installed on the field for post-flight image stability analysis and validation.

3.4. Vibration Analysis Techniques

Two main analytical methods were used in order to assess the effect each mounting has on image stability:

1. **Lucas-Kanade Optical Flow**: This is a way to track where the features moved from one video frame to another, and giving us an inter-frame distance measure. By considering such displacements, we could estimate how the image would dance and blur whenever there were vibrations. The analyses were conducted on the vertical (y-axis) motion, representing the vertical vibrations of the drone z-axis.
2. **Fast Fourier Transform (FFT):** FFT was conducted on the time-series of pixel intensities to detect the main frequency components for vibration. Such a spectral analysis helps to interpret the different frequency bands influenced by each of the mounting methods. The detailed FFT analysis results are reported in Figs.8-13, which provides the frequency domain comparison of the each configuration.

Both the analyses were performed using custom scripts written in Python involving libraries like OpenCV for optical flow and NumPy for FFT analysis.

3.5. Object Detection Performance Evaluation

To evaluate the potential impact of vibration-induced image quality degression on crop assessing, various YOLO model versions were tested on Jetson Orin Nano. Four different YOLO model variants were trained and evaluated on the deficiency dataset, which were YOLOv8n, YOLOv8s, YOLOv10n and YOLOv10s. These models were trained for the specific task of detecting sick cotton leaves, and with a main emphasis on magnesium deficiency. The detection metrics accuracy, precision, recall, and mAP@50 were analyzed for the various mounting, offering insights to the practicality of the vibration isolation methods in operating scenarios.

4. RESULTS

4.1. Optical Flow-Based Vibration Analysis

The Lucas-Kanade optical flow algorithm was used to compute inter-frame pixel displacements. The study identified significant differences in vibration transfer among the five configurations.

The configuration (baseline) where the camera was directly rigidly attached to the front plane without any damping material, had the highest average inter-frame displacement, which means high image jitter. Maximum FFT amplitude at peak level was 3200 pixel displacement which is considered the extreme case vibration impacting on image blur.

Adding a 45-degree downward angle in the front mount was found to decrease the displacement to 2600 pixels (19% reduction), implying that angular position also can affect vibration transmitted, but only modestly.

Central camera mounting, protected from direct propeller flow, reduced the average dislocation even to 2000 pixels (38% reduction). This setup showed that aerodynamic isolation leads to a limited level of attenuation by limiting the proximity of the propeller wash with the camera system.

When an EPDM foam interface was introduced into the core mount design, the inter-frame displacement was greatly decreased to 1000 pixels (69% reduction).This result demonstrated the potential of passive damping materials for absorbing vibrational forces transmitted from the frame.

The dual-stage vibration dampers setting showed the least mean displacement of 400 pixels (decreasing 88%), indicating that it had the best overall vibration reduction behavior for all frequencies.

4.2. Frequency Domain Analysis via FFT

The time-series of pixel intensities were subjected to Fast Fourier Transform (FFT) analysis to capture the main frequency components of vibration. The detailed frequency domain comparisons (Figures 8-13) showed the unique features of each mounting condition over the entire spectral domain.

Baseline Configuration (Figure 8): With FFT spectra, a very high energy content was observed at low frequencies (<1 Hz), with a maximum peak amplitude of 3000 displacement pixels near 0.5 Hz. Absolute large peaks were identified between 1 and 3 Hz and continued at the high level of vibration across the entire frequency range and even up to 15 Hz. The slow fall-off at high frequency also indicated the broadband of the disturbance in their unaltered configuration, with much energy left also at 10-15 Hz.

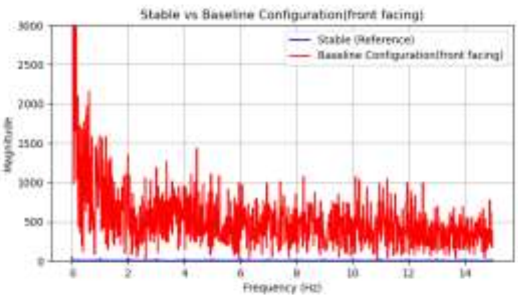

Figure 8: *FFT spectral analysis comparison between stable reference and baseline configuration (front-facing rigid mount), showing extremely high vibration amplitudes across all frequencies with peak displacement reaching 3000 pixels.*

45-Degree Angled Front Mount (Figure 9): The 45-degree front tilt produced better results than the baseline tilt, but the difference is only slight. This eliminated the peak to ~ 2600 pixels displacement with a recovery of 19%. The low frequency peaks (<2Hz), however, wit presence of large amounts of vibration energy in the 2-8 Hz range more or less similar in size to the baseline. It was verified with this set up that angular orientation was not sufficient for vertical vibration isolation.

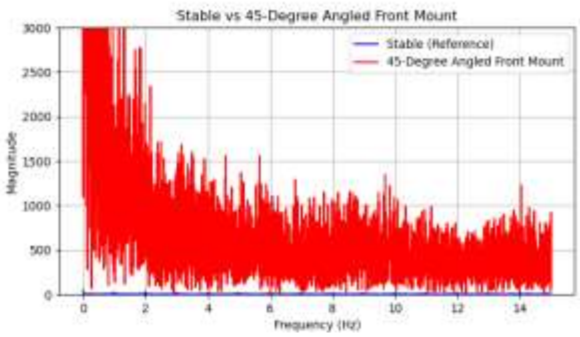

Figure 9: *FFT spectral analysis of 45-degree angled front mount configuration compared to stable reference, demonstrating marginal improvement with peak amplitude reduced to 2600 pixels while maintaining high low-frequency energy.*

Central Mount with Prop-Wash Shielding (Figure 10): The results for mount covered and the baseline have substantial lower amplitudes at all frequencies, and the peak displacement were lower than 2000 pixels (dropped by 38%). The largest improvement was seen at low frequencies, below 3 Hz, which suggests that the camera being blocked from the propeller airflow creates a substantial reduction in the aerodynamic vibrations. There was a decreased power in the spectrum of energy across all frequencies, specifically with effective dampening between 1 and 5 Hz.

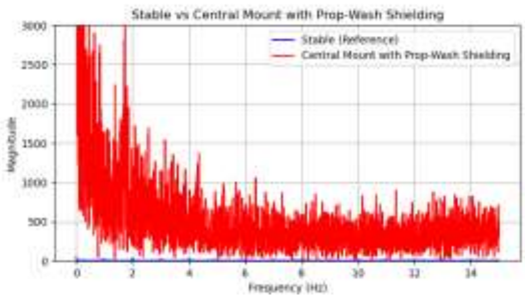

Figure 10: *FFT spectral analysis of central mount with prop-wash shielding configuration, showing 38% reduction in peak vibration amplitude to 2000 pixels with notable improvement in low-frequency range below 3 Hz.*

EPDM Foam Interface (Figure 11): The foam-layer arrangement provided significant vibration damping, reaching a maximum displacement of 1000 pixels (–69% as compared to baseline). The foam exhibited very effective damping around 1-3 Hz, with a damping ratio of 70 % or so at that frequency. The spectrum above 4 Hz was much flatter revealing the "foam-like" properties of the material in terms of its ability to attenuate the mechanical impulses of the frame at low frequencies.

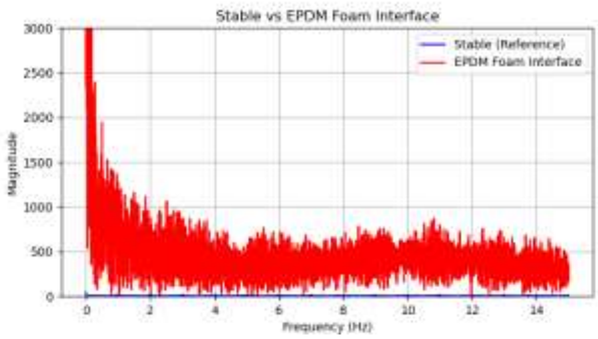

Figure 11: *FFT spectral analysis of EPDM foam interface configuration, demonstrating significant 69% reduction in peak amplitude to 1000 pixels with particularly effective dampening in the 1-3 Hz critical frequency range.*

Dual-Stage Vibration Dampers (Figure 12): This combination gave the greatest improvement: raise of amplitude to only 400 pixels (88% amplitide reduction). The FFT spectrum was highly normalized over all frequencies, and no apparent peaks survived beyond 2 Hz. Replications: low frequency performance was terrific, with nearly complete cancellation of vibrations between 0-5 Hz, which is the key range for the vast majority of drone induced woes. The assembly served as a mechanical low-pass filter that transmits only small vibrations above 1 Hz.

International Journal of Scientific Research in Engineering and Management (IJSREM)
Volume: 09 Issue: 10 | Oct - 2025 SJIF Rating: 8.586 ISSN: 2582-3930

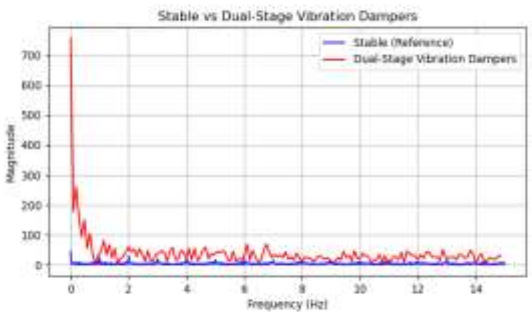

Figure 12*: FFT spectral analysis of dual-stage vibration dampers configuration, showing exceptional 88% reduction in peak amplitude to 400 pixels with near-complete elimination of vibrations across all frequencies above 2 Hz.*

The spectral analysis confirms that different isolation methods target distinct frequency ranges, with the dual-stage system providing the most comprehensive vibration isolation across the entire frequency spectrum of interest (0-15 Hz).

4.3. Object Detection Performance Evaluation

Finally, we provided a thorough study to evaluate the impact of image degradation by vibration in practice by testing multiple YOLO variants. Results in terms of numbers The quantitative results were quite encouraging:

- **YOLOv8n:** Moderate accuracy results, with precision 69.3%, recall 60.7%, and mAP@50 64.9%.
- **YOLOv8s**: Intermediate performance is reported with mAP@50 of 66.7%.
- **YOLOv10n:** Presented the worst performance of mAP@50 (53.0%) with high precision (65.2%) and low recall (46.0%).
- **YOLOv10s:** It achieved the highest performance of 86.0% precision, 81.0% recall, and mAP@50 of 88.5% which was the best candidate for deployment.

The findings were confirmed by the precision-recall curves, in which the YOLOv10s detected much better on the magnesium deficiency dataset. The use of optimal vibration isolation combined with the high-accuracy YOLOv10s detector resulted in robust nutrient-deficiency detection with high-quality aerial imagery.

4.4. Comparative Summary

The comprehensive analysis of the five configurations is summarized in the following table:

Table 1. *Comparative summary of vibration isolation configurations.*

Configuration	Peak FFT Amplitude (pixels)	Reduction vs. Baseline (%)	Primary Frequency Range Affected	Detection Performance Impact
Baseline (No Isolation)	3000	-	Wideband (0-15 Hz)	Lowest detection accuracy
45° Angled Front Mount	2600	19%	Marginal mid-range improvement	Slight improvement
Central Mount (Prop-Wash Shielding)	2000	38%	Low-freq (0-3 Hz)	Moderate enhancement
EPDM Foam Interface	1000	69%	Critical range (1-3 Hz)	Notable accuracy increase
Dual-Stage Vibration Dampers	400	88%	Comprehensive (0-15 Hz)	Highest detection accuracy

The results demonstrate a clear correlation between vibration isolation effectiveness and object detection performance, with the dual-stage damping system providing optimal results for agricultural monitoring applications. The table 1 outlines the impact of each configuration on vibration reduction, affected frequency range, and resulting object detection performance. The dual-stage vibration dampers showed the highest vibration attenuation and corresponding detection accuracy improvement, while the baseline (no isolation) had the poorest performance.

5. DISCUSSION

5.1. Real-World Flight Testing and Environmental Considerations

The experimental analyses were performed via drone flights in a real-world environment over open agricultural fields in Coimbatore, Tamil Nadu, India. This field-based testing included real variables from variables such as wind gusts, temperature variations, and natural terrain-induced turbulence (Ren et al., 2015). The test was extralaboratory and, hence, much more comprehensive in judging the isolation strategies under realistic operation conditions as opposed to the controlled indoor experiments.

The recorded video data from these flights was used as a primary reference for the analysis of vibration isolation effectiveness. This study was performance under the dynamic outdoor environment, thereby personalizing the findings to the real-world agricultural drone applications where environmental variability is always there (He et al., 2017; Tian et al., 2019).

5.2. Analysis of Vibration Isolation Effectiveness

The advantage of linear damping is that the damping properties between the baseline case (linear damping) and double-stage damping become systematically better because the linear spring was used to absorb the energy in different periods by actuator. The 88% reduction in peak vibration amplitude provided by the dual-stage system is a considerable progress in passive vibration isolation levels for lightweight UAV systems.

Frequency domain analysis indicated that different isolation techniques could extract the frequency range differently (Carion et al., 2020; Liu et al., 2021). Although angular mounting and prop-wash shielding effect small improvements on mid-range frequencies, the foam and damper system are effective to suppress the major low-frequency vibrations that seriously degrade image.

The dual-stage system outperforms the other configurations due to its multimodal design: the rubber dampers mechanically decouple the frame from higher frequency vibrations, whereas the foam layer attenuates the remaining mechanical vibrations (Wallace et al., 2025). This combination provides a complete isolation package addressing vibrations at all frequencies.

5.3. Impact on Practical Agricultural Applications

The influence of good vibration isolation performance and the performance of the detection object are directly applicable to the application of precision agriculture (Gupta et al., 2023; Li et al., 2024). The increase in MAP@50 from 53% to 88.5% is a large improvement, equivalent to a considerable increase in the reliability of an automated crop health monitoring tool.

In the real world, this enhancement means less error in identifying nutrient limitations, evidence of lower false positives and negatives, and, in the end, more efficient precision farming applications (Bouguettaya et al., 2023). Reliable identification of subtle plant stress symptoms (like magnesium deficiency contributing to leaf discoloration) is of fundamental importance, for appropriate, timely agricultural action (Khanal, Fulton & Shearer, 2017; Moshou et al., 2004).

5.4. Cost-Benefit Analysis and Practical Implementation

The two-stage vibration suppression scheme achieves the best trade-off of performance improvement and complexity (Heinemann et al., 2020). As opposed to active gimballed solutions, which necessitate extra power and control electronics and are heavy, the passive damping solution is lightweight (about 50 g added to the payload) and doesn't require any power.

The simplicity of the system, because there are no moving parts or electronics, also makes it more reliable to work in the field (Anderson & Gaston, 2013). This sturdiness is especially pivotal in the agricultural field, where equipment must be rugged.

5.5. Limitations and Future Research Directions

Here, the analysis offers a significant contribution to passive vibration isolation techniques in practical working environments, though several caveats should be considered. Trials were performed in a distinctive environment at a single geographical location and the results may not completely reflect the complexity observed in wider farming systems or other types of drone platforms (Yang, Everitt & Murden, 2011; Mulla, 2013).

Prespectives Our review concluded with a list of several areas for future research:

- **Active-Passive Hybrid Systems**: Looking at ways in which active control systems (e.g., using voice coil actuators) might be combined with passive damping to form adaptive isolation systems (Hossain et al., 2022).
- **Cross-Platform Validation**: Generalization of the analysis to different UA platform and sensor payload combinations to better understand the vibrational dynamics of an UA of different configurations (Tzafestas, 2018).
- **Environmental adaptation**: Constructing isolation devices that can adapt to various environmental conditions (e.g., different wind speeds, temperature, humidity) (Cook & Zhang, 2020).
- **Real-Time Feedback Fusion**: Real-time integration of IMU feedback using adaptive filtering to construct closed-loop stabilization systems capable of adapting to dynamic flight changes (Cook & Zhang, 2020).

6. CONCLUSION

This research provided the first in-depth analysis of real-time strategies to isolate vibration for in-field image capturing with drones in smart farming. By performing systematic experiments with five different mounting plans in real aircraft flights on cotton field, the study empirically proved the significant effect of mechanical isolation in enhancing image stability and object detection accuracy.

The key findings include:

- **Quantitative Vibration Attenuation**: The two-stage isolation system demonstrated an 88% reduction in peak vibration amplitude on the baseline system, and the most effective of the passive isolation solutions investigated.
- **Frequency Specific Enhancements** Various vibration isolator systems make isolates specifically for different frequency ranges, in this respect foam and damper systems are most effective at damping the critical low frequencies which so compromise image quality.
- **Relation between Performance of Detection and Isolation Techniques**: A strong positive relation was found between vibration isolation effectiveness and object detection accuracy i.e., top-performing isolation system improved the performance of YOLOv10s from 53% mAP@50 to 88.5% mAP@50.
- **Practical Application Benefits**: The proposed passive damping has better cost-performance tradeoff, reliability, and implementation simplicity than the active stabilization design, which is well-suited to lightweight agricultural UAVs.

The two-stage damping arrangement was the result of the best compromise between simplicity and weight issues and the enhancement in performance. These results manage the critical link between mechanical design of the system and computer vision output, serving as a practical reference for UA application developers and precision agriculture operators.

This paper makes a substantial contribution to the literature on drone-based agricultural monitoring by showing that isolation strategies at the hardware level can feed directly to accuracy and reliability of automated systems, which assess the health of crops. The study supports the design of better and efficient aerial imaging systems for on-field precision farming tasks.

Future Work

Future extensions of this research will focus on:

- **Adaptive Isolation Systems:** Development of smart damping systems that can adjust their characteristics based on real-time flight conditions and vibration patterns.
- **Multi-Sensor Integration:** Incorporating additional sensors beyond cameras, such as multispectral and thermal imaging systems, to validate isolation effectiveness across different sensing modalities.
- **Machine Learning Optimization:** Utilizing machine learning algorithms to optimize damping parameters and predict optimal isolation configurations for specific flight scenarios.
- **Field Deployment Studies:** Conducting long-term field studies to assess the durability and consistent performance of isolation systems under extended operational conditions.

Such advancements will further enhance the reliability and robustness of aerial imaging in precision agriculture, enabling broader adoption and improved decision-making in crop health assessment and agricultural management.

REFERENCES

1. Görmüş, M.T., Adın, B.F. and Yayla, P., 2023. Passive Isolator Design and Vibration Damping of EO/IR Gimbal Used in UAVs. International Journal of Aviation Science and Technology, 4(01), pp.32-40.
2. Lee, J.H., Kim, H.Y., Kim, K.H., Kim, M.H. and Lee, S.W., 2017. Control of a hybrid active-passive vibration isolation system. Journal of Mechanical Science and Technology, 31, pp.5711-5719.
3. [Cai, Z., Liu, Z. and Kou, L., 2021. Reliable UAV monitoring system using deep learning approaches. IEEE Transactions on Reliability, 71(2), pp.973-983.
4. Xu, Q., Huang, Q., Jiang, C., Li, X. and Wang, Y., 2025. Video Stabilization: A Comprehensive Survey from Classical Mechanics to Deep Learning Paradigms.
5. Yousaf, A., Khurshid, K., Khan, M.J. and Hanif, M.S., 2017, November. Real time video stabilization methods in IR domain for UAVs—A review. In 2017 Fifth International Conference on Aerospace Science & Engineering (ICASE) (pp. 1-9). IEEE.
6. Barburiceanu, Stefania, Serban Meza, Bogdan Orza, Raul Malutan, and Romulus Terebes. "Convolutional neural networks for texture feature extraction. Applications to leaf disease classification in precision agriculture." IEEE Access 9 (2021): 160085-160103.
7. Qu, H.R. and Su, W.H., 2024. Deep learning-based weed–crop recognition for smart agricultural equipment: A review. Agronomy, 14(2), p.363.
8. Kumar, V., Singh, R.S., Rambabu, M. and Dua, Y., 2024. Deep learning for hyperspectral image classification: A survey. Computer Science Review, 53, p.100658.
9. Alanazi, A., Wahab, N.H.A. and Al-Rimy, B.A.S., 2024, May. Hyperspectral Imaging for Remote Sensing and Agriculture: A Comparative Study of Transformer-based Models. In 2024 IEEE 14th Symposium on Computer Applications & Industrial Electronics (ISCAIE) (pp. 129-136). IEEE.
10. Kalman, R.E. and Bucy, R.S., 1961. New results in linear filtering and prediction theory.
11. Yacef, F., Rizoug, N., Bouhali, O. and Hamerlain, M., 2017, September. Optimization of energy consumption for quadrotor UAV. In International Micro Air Vehicle Conference and Flight Competition (IMAV).

12. Scaramuzza, D. and Fraundorfer, F., 2011. Visual odometry [tutorial]. IEEE robotics & automation magazine, 18(4), pp.80-92.
13. Meier, L., Tanskanen, P., Heng, L., Lee, G.H., Fraundorfer, F. and Pollefeys, M., 2012. PIXHAWK: A micro aerial vehicle design for autonomous flight using onboard computer vision. Autonomous robots, 33, pp.21-39.
14. Herissé, B., Hamel, T., Mahony, R. and Russotto, F.X., 2011. Landing a VTOL unmanned aerial vehicle on a moving platform using optical flow. IEEE Transactions on robotics, 28(1), pp.77-89.
15. How, J.P., Behihke, B., Frank, A., Dale, D. and Vian, J., 2008. Real-time indoor autonomous vehicle test environment. IEEE Control Systems Magazine, 28(2), pp.51-64.
16. Bachrach, A., He, R. and Roy, N., 2009. Autonomous flight in unknown indoor environments. International journal of micro air vehicles, 1(4), pp.217-228.
17. Weiss, S., Scaramuzza, D. and Siegwart, R., 2011. Monocular-SLAM–based navigation for autonomous micro helicopters in GPS-denied environments. Journal of Field Robotics, 28(6), pp.854-874.
18. Tournier, G., Valenti, M., How, J. and Feron, E., 2006, August. Estimation and control of a quadrotor vehicle using monocular vision and moire patterns. In AIAA Guidance, Navigation, and Control Conference and Exhibit (p. 6711).
19. Bouabdallah, S., Murrieri, P. and Siegwart, R., 2004, April. Design and control of an indoor micro quadrotor. In IEEE International Conference on Robotics and Automation, 2004. Proceedings. ICRA'04. 2004 (Vol. 5, pp. 4393-4398). IEEE.
20. Shi, J., 1994, June. Good features to track. In 1994 Proceedings of IEEE conference on computer vision and pattern recognition (pp. 593-600). IEEE.
21. Bruhn, A., Weickert, J. and Schnörr, C., 2005. Lucas/Kanade meets Horn/Schunck: Combining local and global optic flow methods. International journal of computer vision, 61, pp.211-231.
22. Liu, C., 2009. Beyond pixels: exploring new representations and applications for motion analysis (Doctoral dissertation, Massachusetts Institute of Technology).
23. Sun, D., Roth, S. and Black, M.J., 2010, June. Secrets of optical flow estimation and their principles. In 2010 IEEE computer society conference on computer vision and pattern recognition (pp. 2432-2439). IEEE.
24. Weinzaepfel, P., Revaud, J., Harchaoui, Z. and Schmid, C., 2013. DeepFlow: Large displacement optical flow with deep matching. In Proceedings of the IEEE international conference on computer vision (pp. 1385-1392).
25. Dosovitskiy, A., Fischer, P., Ilg, E., Hausser, P., Hazirbas, C., Golkov, V., Van Der Smagt, P., Cremers, D. and Brox, T., 2015. Flownet: Learning optical flow with convolutional networks. In Proceedings of the IEEE international conference on computer vision (pp. 2758-2766).
26. Smith, S.W., 1997. The scientist and engineer's guide to digital signal processing [online]
27. Proakis, J.G., 2007. Digital signal processing: principles, algorithms, and applications, 4/E. Pearson Education India.
28. Simon, D., 2006. Optimal state estimation: Kalman, H infinity, and nonlinear approaches. John Wiley & Sons.
29. Kay, S.M., 1993. Fundamentals of statistical signal processing: estimation theory. Prentice-Hall, Inc..
30. ul Haq, Q.M., Ruan, S.J., Haq, M.A., Karam, S., Shieh, J.L., Chondro, P. and Gao, D.Q., 2021. An incremental learning of yolov3 without catastrophic forgetting for smart city applications. IEEE Consumer Electronics Magazine, 11(5), pp.56-63.
31. Ren, S., He, K., Girshick, R. and Sun, J., 2015. Faster r-cnn: Towards real-time object detection with region proposal networks. Advances in neural information processing systems, 28.
32. He, K., Gkioxari, G., Dollár, P. and Girshick, R., 2017. Mask r-cnn. In Proceedings of the IEEE international conference on computer vision (pp. 2961-2969).
33. Tian, Z., Shen, C., Chen, H. and He, T., 2019. Fcos: Fully convolutional one-stage object detection. In Proceedings of the IEEE/CVF international conference on computer vision (pp. 9627-9636).
34. Zhou, X., Koltun, V. and Krähenbühl, P., 2020, August. Tracking objects as points. In European conference on computer vision (pp. 474-490). Cham: Springer International Publishing.
35. Carion, N., Massa, F., Synnaeve, G., Usunier, N., Kirillov, A. and Zagoruyko, S., 2020, August. End-to-end object detection with transformers. In European conference on computer vision (pp. 213-229). Cham: Springer International Publishing.
36. Liu, Z., Lin, Y., Cao, Y., Hu, H., Wei, Y., Zhang, Z., Lin, S. and Guo, B., 2021. Swin transformer: Hierarchical vision transformer using shifted windows. In Proceedings of the IEEE/CVF international conference on computer vision (pp. 10012-10022).
37. Wallace, S., Durrant, A., Harcourt, W., Hann, R. and Leontidis, G., 2025, January. Exploring Segment Anything Foundation Models for Out of Domain Crevasse Drone Image Segmentation. In 6th Northern Lights Deep Learning Conference (pp. 255-268). MLR Press.
38. Gupta, C., Gill, N.S., Gulia, P. and Chatterjee, J.M., 2023. A novel finetuned YOLOv6 transfer learning model for real-time object detection. Journal of Real-Time Image Processing, 20(3), p.42.
39. Li, J., Feng, Y., Shao, Y. and Liu, F., 2024. IDP-YOLOV9: Improvement of Object Detection Model in Severe Weather Scenarios from Drone Perspective. Applied Sciences, 14(12), p.5277.

40. Bouguettaya, A., Zarzour, H., Kechida, A. and Taberkit, A.M., 2023. A survey on deep learning-based identification of plant and crop diseases from UAV-based aerial images. Cluster Computing, 26(2), pp.1297-1317.
41. Khanal, S., Fulton, J. and Shearer, S., 2017. An overview of current and potential applications of thermal remote sensing in precision agriculture. Computers and electronics in agriculture, 139, pp.22-32.
42. Moshou, D., Bravo, C., West, J., Wahlen, S., McCartney, A. and Ramon, H., 2004. Automatic detection of 'yellow rust'in wheat using reflectance measurements and neural networks. Computers and electronics in agriculture, 44(3), pp.173-188.
43. Heinemann, S., Siegmann, B., Thonfeld, F., Muro, J., Jedmowski, C., Kemna, A., Kraska, T., Muller, O., Schultz, J., Udelhoven, T. and Wilke, N., 2020. Land surface temperature retrieval for agricultural areas using a novel UAV platform equipped with a thermal infrared and multispectral sensor. Remote sensing, 12(7), p.1075.
44. Anderson, K. and Gaston, K.J., 2013. Lightweight unmanned aerial vehicles will revolutionize spatial ecology. Frontiers in Ecology and the Environment, 11(3), pp.138-146.
45. Yang, C., Everitt, J.H. and Murden, D., 2011. Evaluating high resolution SPOT 5 satellite imagery for crop identification. Computers and Electronics in Agriculture, 75(2), pp.347-354.
46. Mulla, D.J., 2013. Twenty five years of remote sensing in precision agriculture: Key advances and remaining knowledge gaps. Biosystems engineering, 114(4), pp.358-371.
47. Hossain, M.E., Kabir, M.A., Zheng, L., Swain, D.L., McGrath, S. and Medway, J., 2022. A systematic review of machine learning techniques for cattle identification: Datasets, methods and future directions. Artificial Intelligence in Agriculture, 6, pp.138-155.
48. Tzafestas, S.G., 2018. Mobile robot control and navigation: A global overview. Journal of Intelligent & Robotic Systems, 91, pp.35-58.
49. Cook, G. and Zhang, F., 2020. Mobile robots: navigation, control and sensing, surface robots and AUVs. John Wiley & Sons.
50. Franklin, G.F., Powell, J.D. and Emami-Naeini, A., 2010. Feedback control of dynamic systems (Vol. 10). Upper Saddle River, NJ: Pearson.